Acta Crystallographica Section D
Biological Crystallography
ISSN 0907-4449

Three-dimensional atomic structure of a catalytic subunit mutant of human protein kinase CK2

Eugenia Pechkova,[a,b] Giuseppe Zanotti[c,d] and Claudio Nicolini[a,b]*

[a]Fondazione E.L.B.A., Rome, Italy, [b]NanoWorld Institute and Department of Biophysical M&O Sciences Technologies, University of Genova, Italy, [c]Department of Organic Chemistry, University of Padova, Italy, and [d]Venetian Institute for Molecular Medicine, Padova, Italy

Correspondence e-mail: ando@ibf.unige.it

Received 28 March 2003
Accepted 27 August 2003

PDB Reference: human protein kinase CK2, 1na7, r1na7sf.

The three-dimensional crystal structure of the triple-point mutant of the catalytic subunit of human protein kinase CK2α has been determined at 2.4 Å resolution. Microcrystals of mutant CK2 catalytic subunit were obtained by a protein-crystallization method based on thin-film nanotechnology. These microcrystals (of about 20 µm in diameter) were used for diffraction data collection by means of the microfocus beamline at the ESRF synchrotron. A comparison between the human protein kinase CK2α and the corresponding enzyme from a lower organism (*Zea mays*) is made.

1. Introduction

Protein kinase CK2, formerly misnamed casein kinase 2, is a serine/threonine protein kinase that is ubiquitous in eukaryotic organisms (Pinna & Ruzzene, 1996). Despite being one of the first protein kinases to be discovered, its physiological function remains unclear. Much evidence points to the involvement of CK2 in proliferation and tumorogenesis, namely in the phosphorylation of a broad spectrum of endogenous substrates, including oncoproteins and tumour suppressors. CK2 activity indeed appears to be elevated in transformed cells and in solid human tumours (Guerra & Issinger, 1999). Moreover, its deregulated expression in lymphocytes of transgenic mice results in the stochastic production of lymphomas and leukaemia (Seldin & Leder, 1995).

CK2 is generally composed of two subunits, α and/or α' (the catalytic subunits) and β, which combine to form a native $\alpha_2\beta_2$ (or $\alpha'_2\beta_2$ or mixed $\alpha\alpha'\beta_2$) tetramer. Despite this, it lacks a definite form of control: unlike most protein kinases, the catalytic α-subunits of CK2 are in fact constitutively active, either alone or when incorporated into the heterotetrameric holoenzyme. This is quite surprising, particularly if its pleiotropicity is considered (Allende & Allende, 1995). Moreover, its association with regulatory α-subunits may affect the catalytic activity in opposite directions depending on the nature of the substrate (Pinna & Meggio, 1997). Because of these unique properties, the three-dimensional structure of the human CK2α catalytic subunit at the atomic level has biomedical relevance.

The crystal structure of the recombinant catalytic subunit of CK2 from *Zea mays* has been determined (Niefind *et al.*, 1998) both alone and in complex with AMP-PNP and GMP-PNP, two non-phosphorylable analogues of the natural co-substrates (Niefind *et al.*, 1999). Structural studies have also been performed on several complexes of the maize enzyme with inhibitors of halogenated benzimidazoles (Battistutta *et al.*, 2001) and the anthraquinone and xanthenone families

(Battistutta *et al.*, 2000; De Moliner *et al.*, 2003). Moreover, the structure of the dimeric CK2β human regulatory subunit lacking the last 33 residues at the C-terminus tail is known (Chantalat *et al.*, 1999). In contrast, the human CK2α subunit until recently resisted crystallization attempts by traditional vapour-diffusion methods; the reason for this is probably its pronounced overall instability. Furthermore, maize CK2α consists of 332 amino acids, while the human enzyme is 59 amino acids longer at the C-terminus and this long tail is believed to be easily subjected to proteolytic degradation. A low-resolution (3.2 Å) crystal structure of the human holoenzyme has also been determined (Niefind *et al.*, 2001). The human α-subunit in the holoenzyme and the corresponding maize α-subunit appear to be almost totally superimposable; however, owing to this low resolution, fine details of the human CK2α structure may be missed. This is a particularly relevant point since owing to the 70% homology between the two proteins CK2α from *Z. mays* is often used as a model for the human CK2 catalytic subunit studies.

Recently, with the introduction of a new protein-crystallization method based on thin-film nanotechnology (Pechkova & Nicolini, 2001, 2002*a*), we succeeded in crystallizing human CK2α protein kinase and its truncated form (Pechkova & Nicolini, 2002*b*). Here, we present the crystal structure of a triple-point mutant of the catalytic subunit of human recombinant protein kinase CK2α from microcrystals obtained using a homologous protein thin-film template. Owing to the small size of the crystals (about 60 × 20 × 20 µm), diffraction data could only be collected using the Microfocus ID13 beamline at the European Synchrotron Radiation Facility (ESRF, Grenoble) (Cusack *et al.*, 1998).

2. Experimental procedures

2.1. Protein-sample preparation and characterization

A three single-point mutant (Lys10Ser, Glu27Ala, Lys76Asn) of the catalytic α subunit of human CK2 was expressed in *Escherichia coli*. Expression and purification were performed according to the method described by Guerra *et al.* (1998) for CK2α from *Z. mays*.

The CK2α subunit mutant was generated using a QuickChange site-directed mutagenesis kit (Stratagene). Complementary mutagenic oligonucleotides purified by FPLC were utilized. Each mutation was verified by DNA sequencing. The entire nucleotide sequence of the above CK2 triple single-point mutant (Lys10Ser, Glu27Ala, Lys76Asn) is given in Fig. 5(*a*).

Recombinant plasmids for mutant expression were introduced into BL21 *E. coli* cells. The pellet from the culture was resuspended in 25 m*M* Tris–HCl buffer pH 8.5 containing 7 m*M* β-mercaptoethanol. Bacterial lysis was completed by sonicating the bacterial suspension and the extract was centrifuged at 30 000*g* for 20 min. After adjusting the NaCl concentration to 0.2 *M*, the supernatant was loaded onto a phosphocellulose P-11 column (Whatman). A linear salt gradient was applied (0.2–1.5 *M* NaCl) and the elution profile was checked by 12.5% SDS–PAGE. The positive fractions were pooled and loaded onto a heparin–agarose affinity chromatograph. A linear salt gradient (0.5–1 *M* NaCl) was applied and the elution profile was checked spectrophotometrically and electrophoretically. Finally, the eluted fractions were pooled and dialyzed against storage buffer containing 50% glycerol and stored at 253 K.

Functional characterization of the CK2α subunit mutant has been carried out by phosphorylation assay as described by Sarno *et al.* (1998). The activity assay performed points to a 55% reduction of the catalytic activity of the mutant with respect to the wild type.

The triple-point mutant of human recombinant CK2α was concentrated by centrifugation with a Centricon Centrifugal Membrane filter (10 kDa molecular-weight cutoff). The final protein concentration was about 8 mg ml^{-1} in 25 m*M* NaCl, 0.05% NaN_3, 7 m*M* β-mercaptoethanol, 25 m*M* Tris–HCl buffer pH 8.5 (stock solution).

Protein purity after purification and concentration was monitored by SDS–PAGE. The mutant CK2α subunit was analysed using a 12.5% SDS–PAGE gel and proteins were visualized with Coomassie Brillant Blue R-250 (Pechkova & Nicolini, 2002*b*). To monitor the effect of protein degradation, the sample was maintained at 293 K. Degradation bands only appeared after 3 d.

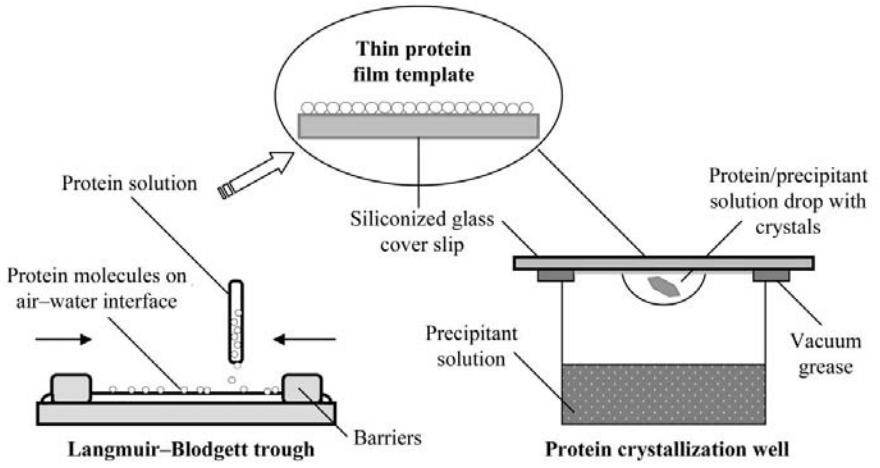

Figure 1
Nanotechnology-based crystallization method utilizing modified hanging-drop vapour diffusion and an homologous protein template produced using a Langmuir–Blodgett trough.

2.2. Microcrystal preparation by a nanotechnology-based template

The Langmuir–Schaefer (LS) template protein-crystallization method (Pechkova & Nicolini, 2001, 2002*a*,*b*) previously introduced is utilized here. As shown in Fig. 1, the proteins were

brought to the air–water interface and then compressed at the desired surface pressure by means of a Langmuir–Blodgett trough (Nicolini, 1997). Surface pressure–area isotherm measurements were performed to characterize the protein monolayer at the air–water interface compressed to 18–20 mN m^{-1}. The transfer of the protein monolayer from the subphase (water or buffer) surface onto a previously siliconized solid (glass) support was performed by touching the support in parallel to the subphase surface according to the LS technique (horizontal lift) (Nicolini, 1997) at the desired protein surface pressure. As shown in Fig. 1, protein nanofilm transferred from the air–water interface onto the siliconized glass cover slide was used as a template in a modification of the classical vapour-diffusion hanging-drop method (Pechkova & Nicolini, 2002*b*). During the crystallization procedure, the following parameters were varied: the precipitant nature and concentration and the number of protein monolayers. In the successful trial, the optimal surface pressure was 20 mN m^{-1}, the number of monolayers was two and a 2 µl drop of stock solution was mixed with 2 µl of precipitant solution (25% PEG 3500, 0.2 *M* sodium acetate, 0.1 *M* Tris pH 8). The drop was equilibrated against a 700 µl reservoir containing the same precipitant solution (25% PEG 3500). Crystals (maximum size 60 × 20 × 20 µm) grew in 3 d at 293 K.

2.3. Data collection

Diffraction data were collected at a temperature of 100 K. Crystals were fished out from the mother liquor and frozen in a nitrogen stream without using cryoprotectant. One needle-shaped crystal of approximate dimensions 60 × 20 × 20 µm was used to collect a complete data set at the Microfocus beamline ID-13 at the ESRF (beam size 20 × 20 µm). The wavelength used was 0.9755 Å and the crystal-to-detector distance was 120 mm. Crystals diffracted to a maximum resolution of 2.4 Å.

CK2α crystals belong to space group $P2_1$, with unit-cell parameters a = 58.68, b = 45.95, c = 63.96 Å, β = 111.8°. One molecule is present in the asymmetric unit. Assuming a molecular mass of approximately 39 000 Da for a truncated protein, the V_M coefficient is about 2.1 Å^3 Da^{-1}, whilst if the molecular mass of the protein is 45 000 Da then V_M becomes about 1.8 Å^3 Da^{-1} (see §3).

2.4. Structure determination and refinement

Data were indexed and integrated with *MOSFLM* (Leslie, 1991) and scaled with the program *SCALA* from the *CCP*4 software package (Collaborative Computational Project, Number 4, 1994). The crystal structure was solved by the molecular-replacement method with the program *AMoRe* (Navaza, 1994), using the structure of the CK2α subunit from *Z. mays* as a template (PDB code 1jam). Crystallographic refinement of the structure was carried out with the *CNS* software package (Brünger *et al.*, 1998), alternated with manual inspection of the electron-density maps and rebuilding of the model using the graphics program *QUANTA* (version 98.1111; Molecular Simulation, Inc). During the final steps of the refinement, 91 water molecules were added in correspondence to electron-density peaks according to the possibility of forming hydrogen bonds with protein atoms or other solvent molecules. The stereochemistry of the final model was checked with the program *PROCHECK* (Laskowski *et al.*, 1993).

Table 1
Data-collection and final model statistics.

Values in parentheses refer to the highest resolution bin.

Beamline	Microfocus ID13, ESRF
Temperature (K)	100
Detector	MAR CCD
Wavelength (Å)	0.9755
Space group	$P2_1$
Unit-cell parameters (Å, °)	a = 58.676, b = 45.954, c = 63.956, β = 111.8
Resolution range (Å)	29–2.40 (2.53–2.40)
Independent reflections	12457 (1817)
Multiplicity	2.3 (2.3)
$\langle I/\sigma(I)\rangle$	4.3 (1.6)
R_{merge}	0.13 (0.37)
Completeness (%)	99.0 (99.4)
Final model	
R	0.209 (0.245)
R_{free}	0.273 (0.0300)
R.m.s. on distances (Å)	0.007
R.m.s. on angles (°)	1.4

Statistics of data collection, processing and refinement are summarized in Table 1. The final model presents an overall R factor of 0.209 (R_{free} = 0.273) with 91 water molecules and a good stereochemistry.

3. Results and discussion

A microcrystal of the triple-point mutant human CK2α protein is shown in Fig. 2. The entire data set utilized to determine the crystal structure was obtained from one microcrystal of dimensions 20 × 20 × 60 µm. The maximum resolution obtained, 2.4 Å, is quite good considering the very small size of the crystal used. A portion of the electron density around residues 152–156 is shown in Fig. 3. The map is generally quite well defined. Residues 5–329 could be located in the map, whilst a short part of the N-terminus (residues 1–4) and the entire C-terminal end (61 residues; 330–390) were not visible.

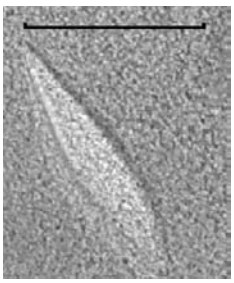

Figure 2
Human CK2α microcrystal obtained using the protein thin-film template method. The scale bar is 40 µm in length.

From our gel-electrophoresis results it would appear unlikely that the protein crystallized is a truncated catalytic subunit; this is suggested by the existence of a very small degradation band which does not appear to change during the purification steps or during the entire process of crystal formation.

Furthermore, the presence of a space in the crystal cell that could accommodate a large part of the C-terminus suggests it could be at least partially present, highly disordered and thereby not visible: in the space left in the proximity of the C-terminus (see Fig. 4*a*) up to 40 alanine residues could indeed be fitted. Another possibility would be that human CK2α has undergone partial proteolytic degradation at the C-terminal end during purification and/or crystallization.

The fractional volume solvent content of the crystal is 31% if the entire molecule is assumed to be present in the asymmetric unit, whilst it increases to about 39% if we consider a truncated protein. In any case, both possibilities strongly suggest that the long C-terminal tail is flexible, at least in the isolated catalytic subunit.

The overall structure of the human CK2α presents the classic fold of the catalytic subunit of protein kinases formed by two domains: an N-terminal domain mainly composed of β-strands and a C-terminal domain which contains several α-helices (Fig. 4*b*). The nucleotide-binding site is located in between the two domains. The structure of the catalytic subunit of the enzyme is similar to that from *Z. mays*, as would be expected from the high sequence homology between the two proteins, at least in the portion we have crystallized (Fig. 5*b*). The overall root-mean-square deviation between equivalent C^{α} atoms of the protein with the maize apoenzyme (PDB code 1jam) is 0.8 Å^2 (Fig. 5*c*). The electron density is generally well defined for main-chain atoms. Breaks in the electron density are present only for residues 72–74 and 122–123. The first break corresponds to the loop that connects strand β3 to helix αC and the amino-acid sequence of this region is identical to that of the maize protein. The beginning of helix αC is believed to be critical for substrate recognition in protein kinases (Pinna & Ruzzene, 1996). The second break is in the first turn of the short helix αD, where some significant differences are present in the amino-acid sequence with respect to that of *Z. mays*:

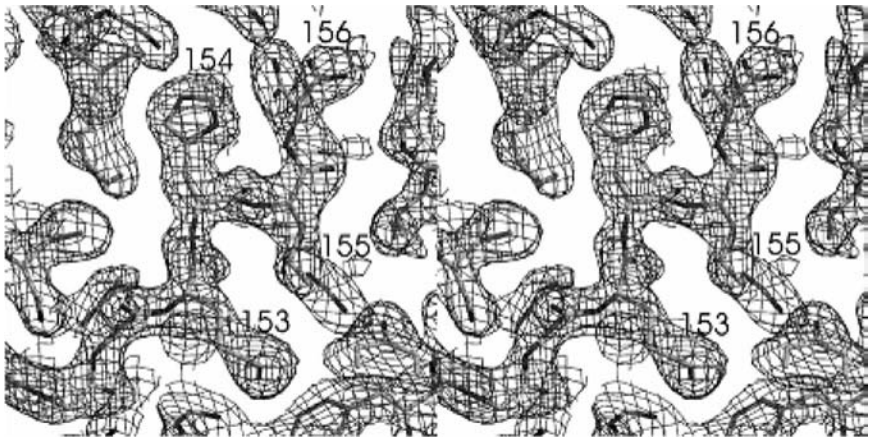

Figure 3
Representation of a portion of the electron-density map, obtained with $|2F_{obs} - F_{calc}|$ coefficients and calculated phases. Contours are drawn at the $1\sigma(\rho)$ level.

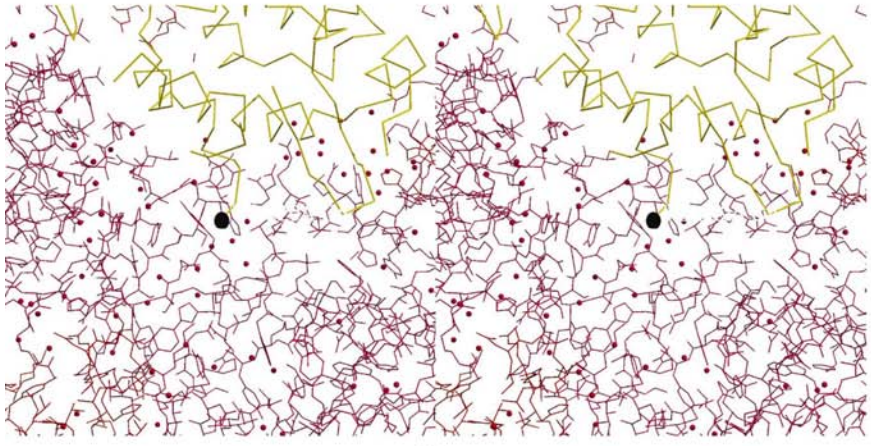

(*a*)

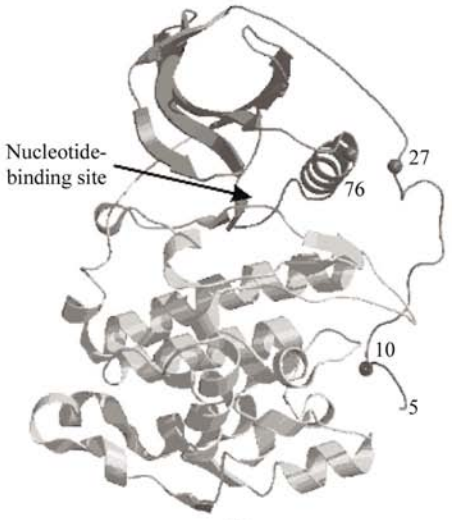

(*b*)

Figure 4
(*a*) Stereographic picture of the C^{α}-chain trace of the reference molecule of the CK2α mutant (yellow lines) along with a symmetry-related molecule in the crystal (magenta lines). Around the C-terminus of the molecule (black label) there is space available for a disordered C-terminal chain. Water molecules are shown as magenta spheres. (*b*) Cartoon representation of the three-dimensional atomic structure of human CK2α. The N-terminal domain is in dark grey and the C-terminal domain is in light grey. Spheres mark the positions of the three point mutations.

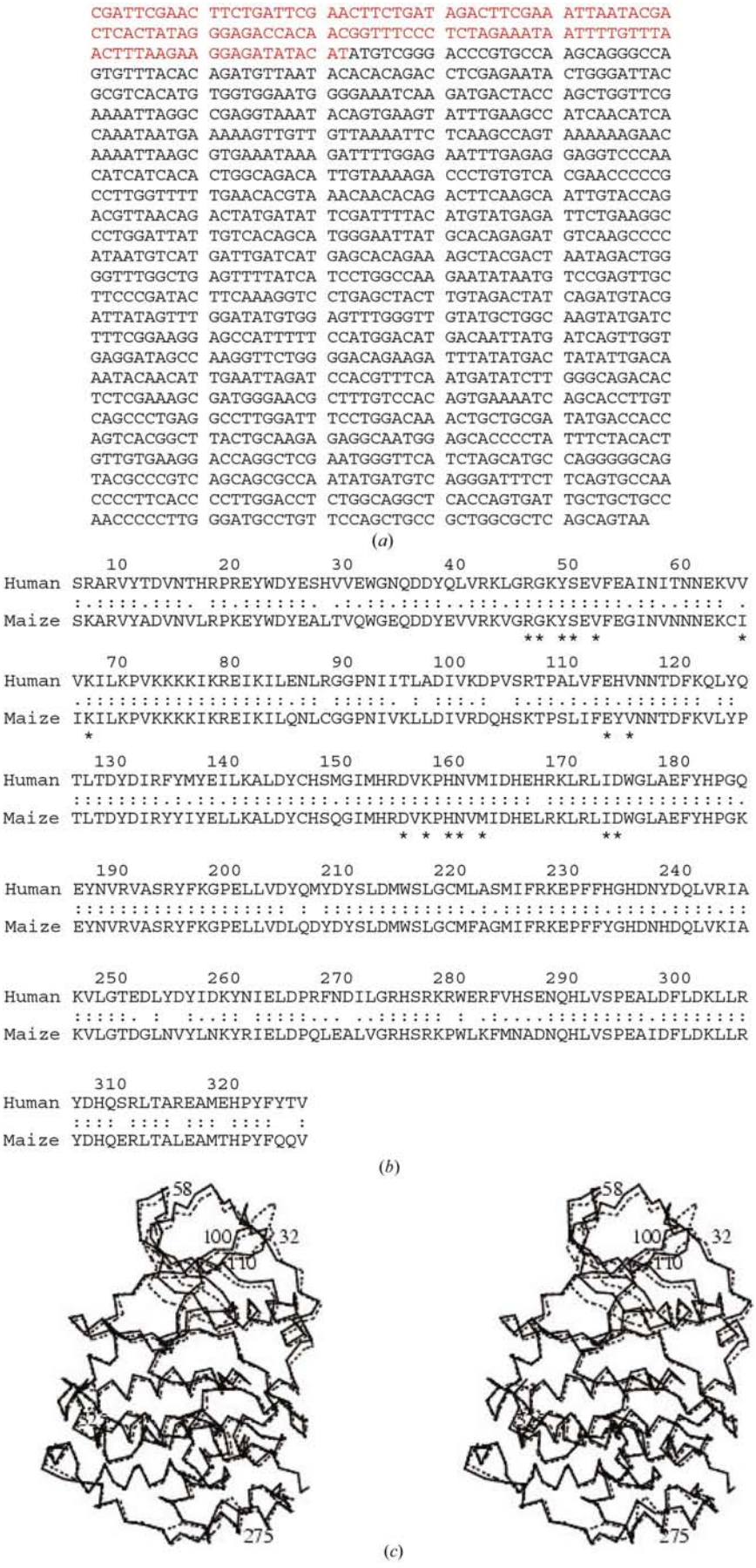

residue 123 is a Gln instead of a Val and Gln26 substitutes a Pro, possibly inducing a perturbation of the structure.

The most significant conformational differences between the human and the maize protein are present mainly in the N-terminal domain; in particular, residues 102–109, *i.e.* the loop connecting strands $\beta4$ to $\beta5$, and the area containing residues 40–57. The latter is particularly relevant, since it contains the so-called Gly-rich loop (residues 42–50; Niefind *et al.*, 1998); moreover, some of these residues directly interact with the nucleotide when it is bound to the protein. Conformational differences in this loop have been observed previously for the maize protein, either in the apo form or in some of its complexes with inhibitors (Battistutta *et al.*, 2001). Overall, the structure of the C-terminal domain is better preserved, a fact that was observed in all the crystal structures of protein–inhibitor complexes determined to date. The three point mutations have no apparent structural effect, since the secondary structure around residues 10, 27 and 76 is completely conserved with respect to the maize protein. A comparison with the catalytic subunit of the human protein in the $\alpha_2\beta_2$ complex yields similar conclusions, although the latter structure is at relatively low resolution.

No ATP or analogues were added during the crystallization process. An examination of the nucleotide-binding site cavity shows no density at all, indicating that the protein we have crystallized is in the apo form. The superposition of the co-substrate binding-site cavities in the human and maize proteins is illustrated in Fig. 6, where it is evident that they are very similar. Residues

Figure 5
(*a*) Nucleotide sequence of CK2α triple single-point mutant (Lys10Ser, Glu27Ala, Lys76Asn). The vector pT7-7 is indicated in red. (*b*) Alignment of the amino-acid sequences of the catalytic subunit of human and maize protein kinase CK2. The identity is 77.6% for a 321-amino-acid superposition. Stars indicate residues that possess at least one atom which is a distance shorter than 3.9 Å from the nucleotide analogue AMP-PNP, as calculated from coordinates taken from Niefind *et al.* (1999). The numbering system used is that of the human protein. The alignment was obtained with the program *LALIGN* (Huang & Miller, 1991). (*c*) Superposition of the C$^{\alpha}$-chain trace of the human protein (continuous line; PDB code 1na7) on the apo form of *Z. mays* CK2α (dashed line; PDB code 1jam).

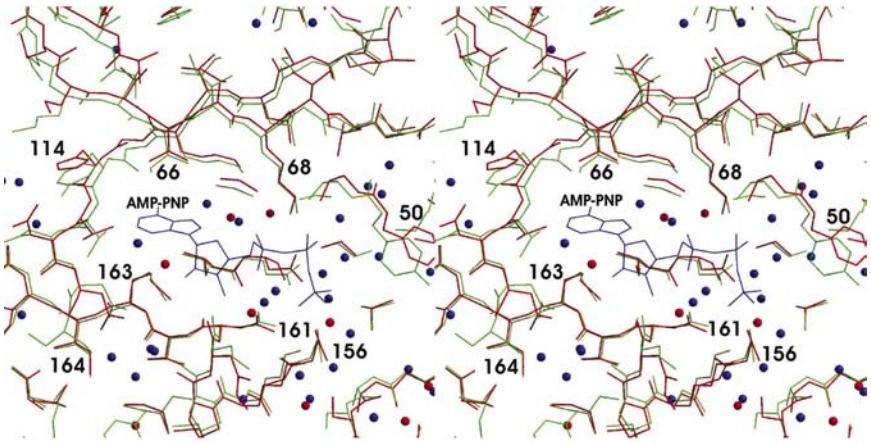

Figure 6
Superposition of the active sites of the human CK2 catalytic subunit (red) on the holo form of *Z. mays* CK2 (green) (Battistutta *et al.*, 2000). The ATP analogue (phosphoamino phosphonic acid-adenylate ester) bound to the holo CK2 crystal structure is shown in blue.

close to the nucleotide are indicated by a star in Fig. 5(*b*). They are all conserved, with the exception of Ile66 which is a Val in the human enzyme, but the latter substitution has apparently no effect on the co-substrate interaction with the protein. The only non-conservative substitution that takes place in the proximity of the nucleotide-binding site is His115, which is substituted by a Tyr in the maize protein. The OH group of Tyr115 forms a hydrogen bond with the side chain of Asn117, but in the human protein the latter moves slightly in order to accommodate the same kind of interaction with His115. Minor differences in side-chain positions in the human enzyme are more likely to be attributable to the absence of any ligand in the co-substrate cavity rather than to real differences between the two proteins.

Several water molecules are present in the active-site pocket. In particular, two of them seem to be relevant for the active-site conformation, since they are invariably present in all the structures of the maize enzyme solved to date (Battistutta *et al.*, 2001), with the exception of the CK2α–emodin complex (Battistutta *et al.*, 2000). They are also present in human CK2α, one of them being hydrogen bonded to one of the O atoms of the carboxyl group of Glu81 (W4—OE2Glu81, 3.12 Å) and the other interacting with the first one (W4—W59, 3.20 Å).

4. Conclusions

The crystal structure of the catalytic subunit mutant of human CK2α at 2.4 Å resolution reported in this paper and deposited in the Protein Data Bank on 27 November 2002 (PDB code 1na7) confirms the idea that the molecular models of the human and maize proteins are very similar (Pechkova, 2003). This similarity, which is particularly pronounced as far as the active sites are concerned and which was subsequently confirmed by a structure of truncated human CK2α (PDB code 1pjk, deposited on 24 June 2003; Ermakova *et al.*, 2003), supports the validity of the previous use of the maize protein as a model for the human protein. The similarity between two species that are evolutionary so distant could possibly be related to a conservation of physiological function. A distinctive feature of the catalytic α-subunit of the human enzyme is that it has a C-terminal tail that is significantly longer and more flexible with respect to the maize protein and to human α'. In this respect, one could speculate that it is human α' and not α that is the homologue of the maize protein. Consequently, the structural similarity between the human α and that from *Z. mays* further support the hypothesis of a strong structural similarity between the two forms of the enzyme.

The similarity of the human and maize proteins particularly near their active sites enhances the pharmacological relevance of all the binary complexes of maize CK2 with inhibitors that have been obtained.

Finally, it is noticeable that very small crystals in conjunction with the use of a microfocus beamline of a third-generation synchrotron can give a 2.4 Å resolution comparable to or better than that obtained with crystals of much larger size on a conventional X-ray source (Pechkova & Nicolini, 2003).

We are grateful to the beamline staff of ID13 at ESRF/EMBL, Grenoble, Christian Riekel, Manfred Burghammer and David Flot, for excellent conditions and support during data collection. We would also like to thank Roberto Battistutta for help during the crystallographic refinement process. This and related work was entirely supported by an FIRB grant from the Italian Ministry of Education, Research and Universities to the Fondazione E.L.B.A.

References

Allende, J. E. & Allende, C. C. (1995). *FASEB J.* **9**, 313–323.
Battistutta, R., De Moliner, E., Sarno, S., Zanotti, G. & Pinna, L. A. (2001). *Protein Sci.* **10**, 2200–2206.
Battistutta, R., Sarno, S., De Moliner, E., Papinutto, E., Zanotti, G. & Pinna, L. A. (2000). *J. Biol. Chem.* **275**, 29618–29622.
Brünger, A. T., Adams, P. D., Clore, G. M., DeLano, W. L., Gros, P., Grosse-Kunstleve, R. W., Jiang, J.-S., Kuszewski, J., Nilges, M., Pannu, N. S., Read, R. J., Rice, L. M., Simonson, T. & Warren, G. L. (1998). *Acta Cryst.* D**54**, 905–921.
Chantalat, L., Leroy, D., Filhol, O., Nueda, A., Benitez, M. J., Chambaz, E. M., Cochet, C. & Dideberg, O. (1999). *EMBO J.* **18**, 2930–2940.
Collaborative Computational Project, Number 4 (1994). *Acta Cryst.* D**50,** 760–763.
Cusack, S., Bernali, H., Bram, A., Burghammer, M., Perrakis, A. & Riekel, C. (1998). *Nature Struct. Biol.* **5**, 634–637.
De Moliner, E., Moro, S., Sarno, S., Zagotto, G., Zanotti, G., Pinna, L. A. & Battistutta, R. (2003). *J. Biol. Chem.* **278**, 1831–1836.
Ermakova, I., Boldyreff, B., Issinger, O.-G. & Niefind, K. (2003). *J. Mol. Biol.* **330**, 925–934.
Guerra, B. & Issinger, O.-G. (1999). *Electrophoresis*, **20**, 391–408.
Guerra, B., Niefind, K., Pinna, L. A., Schomburg, D. & Issinger, O.-G. (1998). *Acta Cryst.* D**54**, 143–145.

Huang, X. & Miller, W. (1991). *Adv. Appl. Math.* **12**, 373–381.
Laskowski, R. A., MacArthur, M. W., Moss, D. S. & Thornton, J. M. (1993). *J. Appl. Cryst.* **26**, 283–291.
Leslie, A. G. W. (1991). *Crystallographic Computing*, edited by D. Moras, A. D. Podjarny & J. P. Thierry, pp. 27–38. Oxford University Press.
Navaza, J. (1994). *Acta Cryst.* A**50**, 157–163.
Nicolini, C. (1997). *Trends Biotechnol.* **15**, 395–401.
Niefind, K., Guerra, B., Ermakova, I. & Issinger, O.-G. (2001). *EMBO J.* **20**, 5320–5331.
Niefind, K., Guerra, B., Pinna, L. A., Issinger, O.-G. & Schomburg, D. (1998). *EMBO J.* **17**, 2451–2462.
Niefind, K., Putter, M., Guerra, B., Issinger, O. G. & Schomburg, D. (1999). *Nature Struct. Biol.* **6**, 1100–1103.
Pechkova, E. (2003). PhD Dissertation. University of Genova, Italy.
Pechkova, E. & Nicolini, C. (2001). *J. Cryst. Growth*, **231**, 599–602.
Pechkova, E. & Nicolini, C. (2002*a*). *Nanotechnology*, **13**, 460–464.
Pechkova, E. & Nicolini, C. (2002*b*). *J. Cell Biochem.* **85**, 243–251.
Pechkova, E. & Nicolini, C. (2003). *Proteomics and Nanocrystallography*, pp. 1–210. Dordrecht: Kluwer Academic Publishers.
Pinna, L. A. & Meggio, F. (1997). *Prog. Cell Cycle Res.* **3**, 77–97.
Pinna, L. A. & Ruzzene, M. (1996). *Biochim. Biophys. Acta*, **1314**, 191–225.
Sarno, S., Marin, O., Ghisellini, P., Meggio, F. & Pinna, L. A. (1998). *FEBS Lett.* **441**, 29–33.
Seldin, D. C. & Leder, P. (1995). *Science*, **267**, 894–897.